Parametric representation of Stiles–Crawford functions: normal variation of peak location and directionality

Raymond A. Applegate

Department of Ophthalmology, The University of Texas Health Science Center at San Antonio, 7703 Floyd Curl Drive, San Antonio, Texas 78284-6230

Vasudevan Lakshminarayanan

Allergan Therapeutics, Surgical R, D, and Engineering, Clinical Research Group, 9701 Jeronimo Road, Irvine, California 92718, and Department of Cognitive Science, School of Social Sciences, University of California at Irvine, Irvine, California 92717

Received August 21, 1992; revised manuscript received January 11, 1993; accepted January 11, 1993.

Evidence suggests that the psychophysically determined Stiles–Crawford effect of the first kind (SCE) reflects waveguide properties of human photoreceptors. The peak of the SCE data set is assumed to reflect the principal alignment tendencies, and the spread (e.g., ρ value, the curvature or width at half-height) is assumed to reflect the directionality (i.e., interreceptor differences in alignment) of the population of photoreceptors being tested. As such, disruption of the normal SCE can be used and/or has been used (1) to document early natural history of retinal pathology involving the photoreceptors, (2) to provide a firm rationale for therapeutic intervention, and (3) to provide a method for monitoring therapies designed to alter the natural course of retinal-disease processes. We report large-sample norms for foveal SCE peak location and spread (horizontal peak location, nasal 0.51 ± 0.72, horizontal ρ value 0.047 ± 0.013, vertical peak location, superior 0.20 ± 0.64, vertical ρ value 0.053 ± 0.012), compare these norms with values determined in other laboratories, and discuss the various mathematical forms used for the empirical description of SCE data sets.

INTRODUCTION

The Stiles–Crawford effect of the first kind (SCE) was first reported in 1933.[1] Simply stated, the SCE is the experimental observation that light entering near the center of the pupil is more efficient in eliciting a visual response than is light entering peripheral regions of the pupil (Fig. 1). Subsequent research in several laboratories has demonstrated the effect to be retinal in origin and best explained as a direct consequence of the waveguide properties of the photoreceptors considered as fiber-optic elements. Reviews of the evidence supporting these conclusions are presented in Ref. 2 and in a more recent review chapter by Enoch and Lakshminarayanan.[3] The principal evidence supporting the photoreceptor-waveguide explanation of the SCE and its relevance to retinal and visual function includes the findings that (1) the SCE cannot be accounted for by preretinal reflection and/or absorption[1,4,5]; (2) the magnitude of the SCE is markedly reduced under scotopic conditions[6,7]; (3) the magnitude of the SCE is altered with changes in receptor morphology[8]; (4) the SCE is evident in measures of retinal densitometry[9–12]; (5) neighboring receptors are nearly parallel and, throughout the retina, orient their long axes toward the center of the eye's exit pupil[13]; (6) the SCE recovers after disruption by normal[14] and pathological[15–18] retinal stress; and (7) the peak location of the SCE actively shifts with changes in pupil location.[19,20]

It is the consensus that the peak of the SCE estimates the principal alignment tendencies of the population of photoreceptors being tested and that the spread or width of the SCE reflects the directionality (interreceptor differences in alignment) of the population photoreceptors being tested. To define the peak location and width of the SCE objectively, single traverse-data sets [circles, Fig. 2(a)] of relative retinal sensitivity across a central horizontal or vertical pupillary meridian [Fig. 2(b)] are generally fitted with a describing function by use of least-squares-fitting techniques [curve, Fig. 2(a)], and the calculated coefficients of the best-fit curve are used to define the principal alignment tendencies (peak location) and the directionality (the width of the curve) objectively.

EMPIRICAL DESCRIPTION OF STILES–CRAWFORD DATA

A number of mathematical functions have been proposed for fitting the photopic SCE data.[6,21–26] These functions are generally of the form $\eta = f(x)$, where η is a measure of the relative luminous efficiency (defined as the ratio of the luminance of a fixed standard entering the pupil from a fixed central location and the luminance of a displaced test beam) as a function of test-beam location within the entrance pupil of the eye.

First proposed and used by Stiles,[21] the most commonly used function for fitting experimentally obtained SCE data sets is that of a second-order polynomial, a parabola [Eq. (1)]. A parabola is an excellent fit to an SCE data set obtained from sampling a single pupillary meridian (e.g.,

0740-3232/93/071611-13$06.00

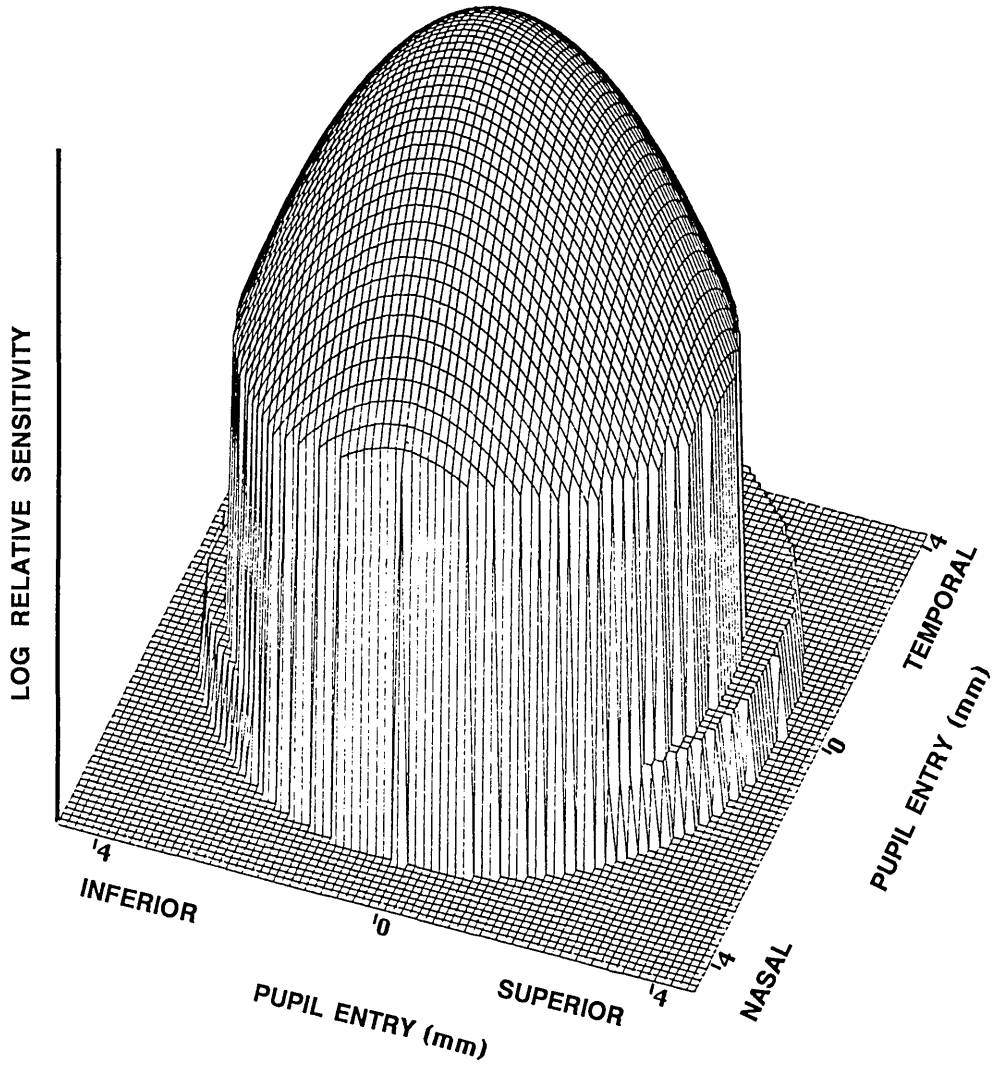

Fig. 1. Idealized model of the SCE within the eye's pupil graphically displayed as log relative sensitivity as a function of pupil entry. The circular pedestal represents the dilated 8-mm pupil. Notice that the peak SCE is slightly nasal (0.50 mm) and superior (0.20 mm) to the pupil center.

horizontal or vertical meridian) as long as the fitted data are limited to ±3 mm of the data set's peak and the data are reasonably symmetric about the peak. Stiles's function is given by

$$\eta = \eta_{max} 10^{-\rho(x - x_{max})^2}, \tag{1}$$

or, if one takes logarithms of both sides,

$$\log \eta = \log \eta_{max} - \rho(x - x_{max})^2, \tag{1a}$$

where η is a measure of sensitivity at a given pupil-entry position, $(x - x_{max})$ is a measure of the distance in the entrance pupil of the eye (in millimeters) from the location of the peak of sensitivity (η_{max}), and ρ is the shape factor (related to peakedness or curvature and hence the width or spread of the curve). Figure 3 shows a family of parabolas generated by use of Eq. (1) that vary in ρ value. Note that as ρ increases, the function is more peaked (or less flat).

Typical SCE data fitted with a parabolic function yield progressively smaller estimates of ρ as points farther from the function peak are included in the analysis. The parabolic relationship begins to fail markedly when one includes data points that are greater than ±3 mm from η_{max}.[1] Despite this limitation, a significant asset of the parabolic fit is the fact that, if the two-dimensional SCE is a solid parabola (as in Fig. 1), the ρ value is a constant even if the sample traverse does not pass through the true SCE peak.[27]

It should be noted that the most general parabolic relationship can be written as

$$y = ax^2 + bx + c. \tag{2}$$

This is a more convenient form of the equation for a parabola, which can be readily programmed even into a hand calculator. If one compares Eq. (1a) with Eq. (2), it can be readily seen that the coefficients of Stiles's equation are defined by the general parabolic equation as

$$\rho = -a,$$
$$x_{max} = -(b/2a),$$
$$\log \eta_{max} = c - (b^2/4a). \tag{2a}$$

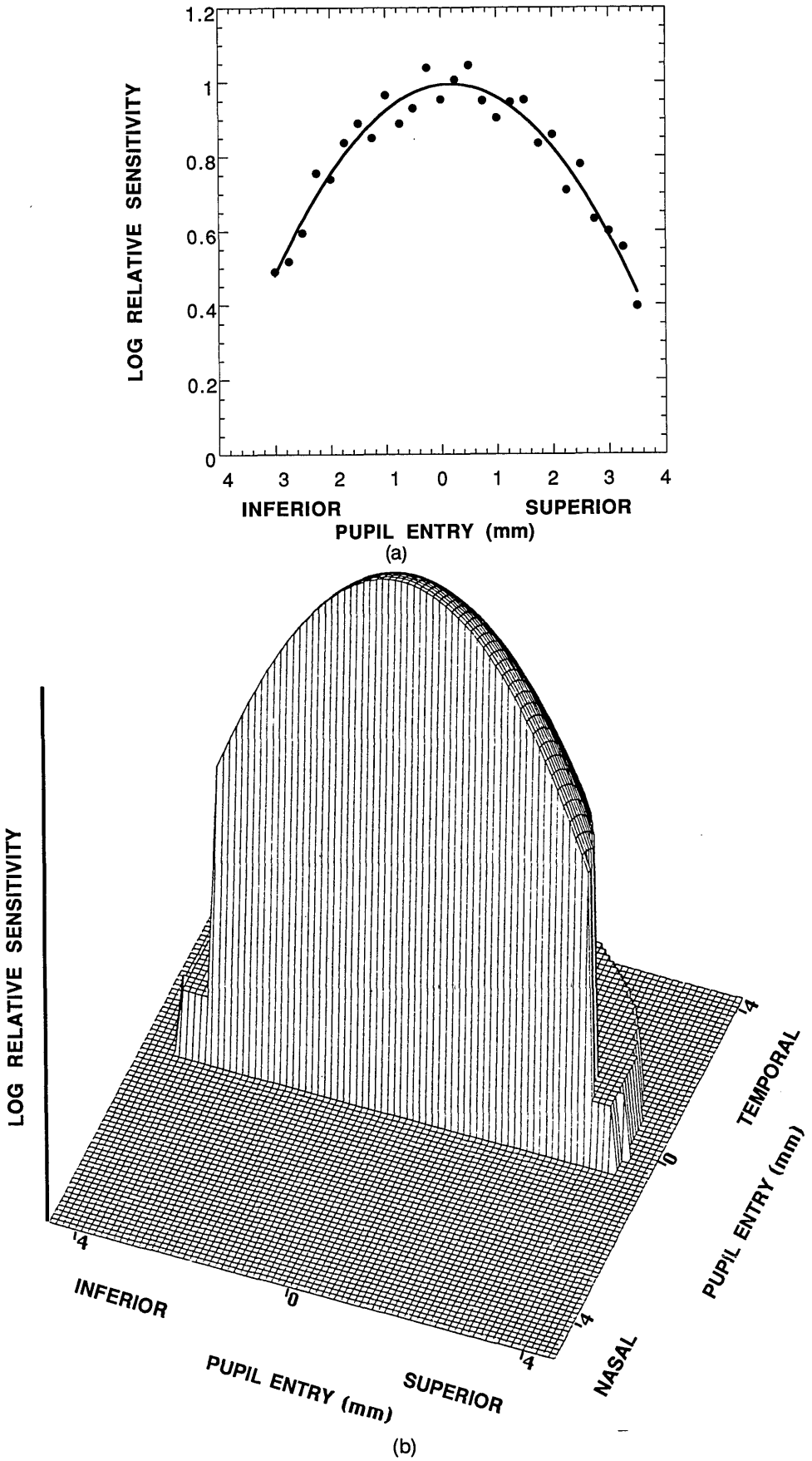

Fig. 2. (a) Typical graphical representation of the SCE illustrating that sensitivity is measured experimentally at discrete pupillary locations along a single pupil traverse (data points) and best fit with a describing function (curve). (b) Cross section of Fig. 1 illustrating that the SCE is quantified by psychophysically measuring the log relative sensitivity along a single central meridian.

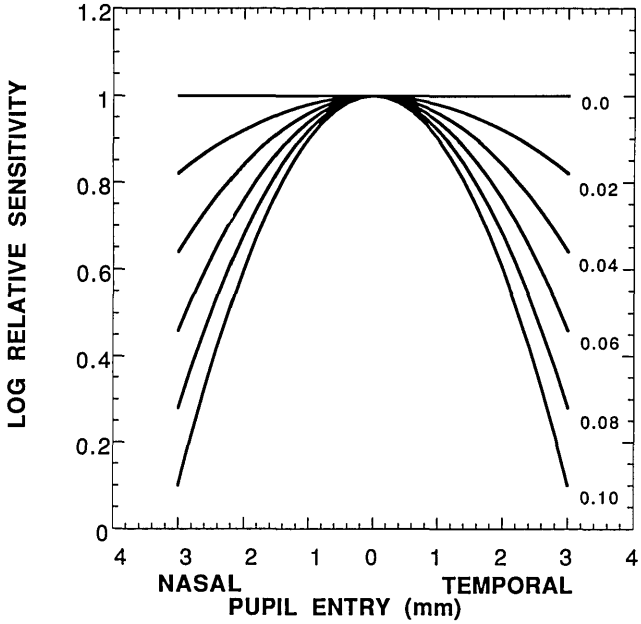

Fig. 3. Parabolic curves illustrating changes in sensitivity for ρ parameters ranging between 0.000 (a line) and 0.100. A typical foveal ρ value for either horizontal or vertical SCE data sets is ~0.050.

In both formulations the independent variable is pupil-entry position (generally expressed in millimeters) and the dependent variable is luminous efficiency (generally expressed as log η or an equivalent). As a historical note, Moon and Spencer,[22] in addition to using a parabola to describe SCE data empirically, also used an equation of the form

$$\eta = (1 - a) + a \cos bx. \tag{3}$$

If one uses a series expansion of the cosine (or equivalently a sine term with a phase term), Eq. (3) can be written as

$$(1 - a) + a \cos bx$$
$$= (1 - a) + a[1 - b^2x^2/2! + b^4x^4/4! - \ldots]$$
$$= 1 - (ab^2/2!)x^2 + (ab^4/24)x^4 - \ldots.$$

With proper choice of the coefficients a and b and by neglecting higher-order terms, the cosine expansion can be represented by a parabolic equation. Enoch[23] used a function of the form

$$\eta = A(1 + \cos B\theta)^2,$$

where A and B are suitable constants and θ is the angle at which a ray of light strikes the retina. (For the Gullstrand exact schematic eye, 2.5 deg equals ~1-mm beam displacement in the plane of the exit pupil of the phakic eye.[28]) If the above expression is simplified and higher-order terms are deleted, the result is an essentially parabolic form:

$$\eta = 4 - 1.5B^2\theta^2 + (1/6 + B^2/4)B^2\theta^4.$$

The point to note is that these functions represent empirically determined truncated cosine (or sine) expansions and are not generally used to describe SCE data sets.

Safir and Hyams[24] and Safir *et al.*,[25,29] using Gaussian functions to fit SCE data sets, demonstrated that the Gaussian gives a statistically better fit to foveal SCE data than does a parabola [Fig. 4(a)], especially when peripheral pupillary points are included (more than ±3 mm from the peak of the SCE). They reported that over the fully dilated pupil the parabolic representation was statistically rejected at the 95% confidence level and the Gaussian function was more appropriate. However, if the data set used to fit the function is limited to ±3 mm from the peak, the Gaussian fit is only slightly better than a parabolic fit [Fig. 4(b)]. The general form of the function used by Safir is

$$\log \eta - K_1 = K_2 + A \exp[-B(x - c)^2]. \tag{4}$$

Here c is a centering constant (location of the peak), K_2 is the horizontal asymptote, K_1 is an arbitrary constant that depends on the optics of the apparatus used to measure the data set, and A and B are parameters of the spread. Similar Gaussian functions have been used by Crawford[6] and Geri *et al.*[26]

Despite the fact that the Gaussian fit better represents SCE data set over the entire pupil, the Stiles formula (or equivalent parabolic relationship) is used almost exclusively today as the describing function to quantify objectively SCE data sets ±3 mm from the peak of the effect.

Alternative Specification of Receptor Directionality

Enoch and Bedell[30] have proposed that directionality be specified in terms of the distance in the pupil, relative to the function peak at which relative luminous efficiency (η) falls to one half of the maximum or peak value (i.e., a decrease of 0.30 log unit from the peak value when the data are plotted in logarithmic ordinates). The underlying physical analogy is that retinal cones can act as dielectric antennae, as was first pointed out by Toraldo di Francia[31] in his interpretation of SCE data. This value would correspond to the half-power point or angle. Similarly, Enoch[32] and Tobey *et al.*[33] pointed out that a half-sensitivity half-width may be defined that can be applied to the far-field radiation patterns of photoreceptors, further establishing the connection between psychophysically obtained SCE data and the waveguide properties of photoreceptors. In addition to reinforcing the underlying physical analogy, another advantage is that the half-sensitivity points would lie within the central area of the photopic SCE function, where the data are well fitted by any of the empirical forms discussed above. Enoch and Bedell[30] provided a table of conversion between directionality expressed in terms of the Stiles parameter and the half-sensitivity half-width. If one is analyzing data fitted with Gaussian functions of the form of Eq. (4), then the half-width from such a fit can be directly compared with the conventional directional-sensitivity parameter ρ by using the relationship

$$\text{half-width} = (0.30/\rho)^{1/2}. \tag{5}$$

Interpreting Changes in SCE Peak Location and ρ Value

As discussed above, the peak of the SCE data set is assumed to reflect the principal alignment tendencies, and the spread is assumed to reflect the directionality of the

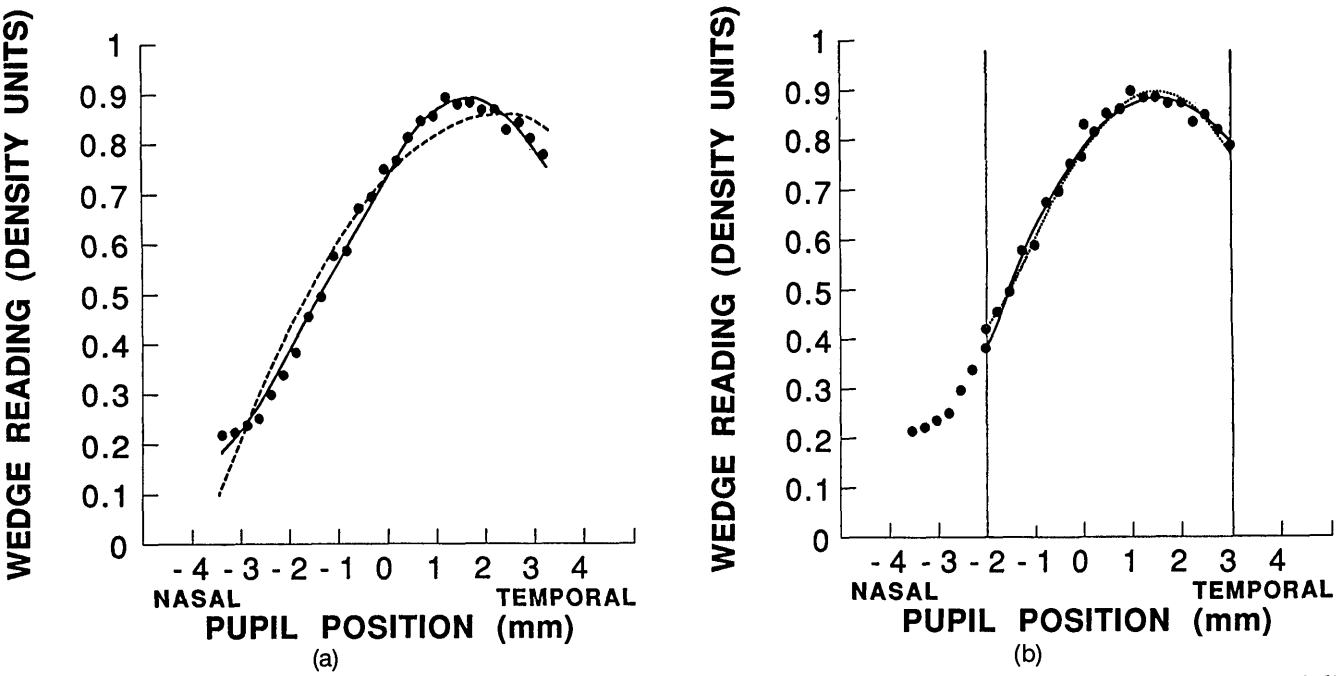

Fig. 4. (a) Figure 7 from Ref. 24, illustrating that a Gaussian curve (solid curve) is a better fit to the data (circles) than is a parabolic curve (dashed curve). (b) Figure 8 from Ref. 24, illustrating that both the Gaussian (solid curve) and parabolic (dashed curve) fit are good representations of the SCE data set (circles) when the data set considered is limited to ±3 mm from the peak of the SCE.

population of photoreceptors being tested. Although changes in SCE peak location in pathology or trauma can be accounted for by a change in the alignment tendencies of the photoreceptors being tested,[2,3,34] a decrease in ρ value in pathology can be explained in at least three ways: The variability of photoreceptor alignment has increased (e.g., there is receptor splaying, possibly because of retinal traction or subretinal fluid accumulation), there is a change in the photoreceptor's optical bandwidth (acceptance angle), or there is an increase in light leakage between neighboring receptors. Although the third possibility, light leakage, is plausible, it is unlikely to affect the outcome. Theoretical studies[35] on absorbing optical waveguides show that such a leak is not likely to lead to a significant attenuation in the transmission of energy down the photoreceptor. It is worth noting that it may be possible to differentiate between the first and second possibilities by using selective adaptation techniques.[36] Specifically, by using selective adaptation and assuming that light leakage between receptors remains constant, it has been shown that photoreceptors in the fovea are splayed in gyrate atrophy[37] but not in retinitis pigmentosa,[38,39] even though both sets of patients exhibited similar flattened SCE functions. Furthermore, it has been shown that the selective-adaptation paradigm is robust and can be used even in cases of mild cataract.[40] Thus both SCE peak location and ρ value are useful in detecting photoreceptor involvement and in giving insight to physical changes in the receptors themselves.

SCE: Two-Dimensional Nature

Most previous investigations have reported SCE data for a central horizontal meridian and have assumed that the function is two-dimensionally symmetric as illustrated in Fig. 1. The assumption of two-dimensional symmetry of an SCE measured along a single central pupillary meridian can lead to erroneous conclusions, particularly in abnormal eyes. To illustrate this point, consider the SCE illustrated in Figs. 5 and 6. Figure 5(a) illustrates a central horizontal SCE data set from a subject that has an apparently flat ρ value.[41] If data collection were limited to this data set alone, one could draw the conclusion that this eye has little retinal directional sensitivity. Figure 5(b) displays this same subject's SCE for the vertical pupillary meridian. Notice that in the vertical pupillary meridian the eye demonstrated strong directional sensitivity with a markedly displaced SCE peak location. By sampling a total of seven different pupillary meridians across the pupil, a two-dimensional contour map of log relative sensitivity as a function of pupil entry can be constructed to illustrate retinal sensitivity across the pupil [Fig. 6(a)]. In Fig. 6(a) contour lines represent pupil-entry locations of equal sensitivity, and the horizontal and vertical lines represent the pupil locations sampled in the horizontal and vertical pupillary meridian illustrated in Figs. 5(a) and 5(b). Notice that the location of the actual peak of the SCE is inferior and slightly nasal and that in this case sampling two orthogonal meridians reasonably locates the SCE peak but leaves uncertainty to the actual spread of the effect when the pupillary meridian(s) sampled miss the SCE peak location by a relatively large amount. Figure 6(b) redisplays the contour map as a three-dimensional sensitivity surface that permits easy visualization of the eye's directional sensitivity and the problems associated with sampling a single pupillary meridian. Interestingly, this subject had 20/25 best-corrected visual acuity and no known systemic or retinal pathology.

Description of the SCE in the Presence of Cataract

Cataracts severely complicate the interpretation of the measured SCE when one is attempting to study receptor

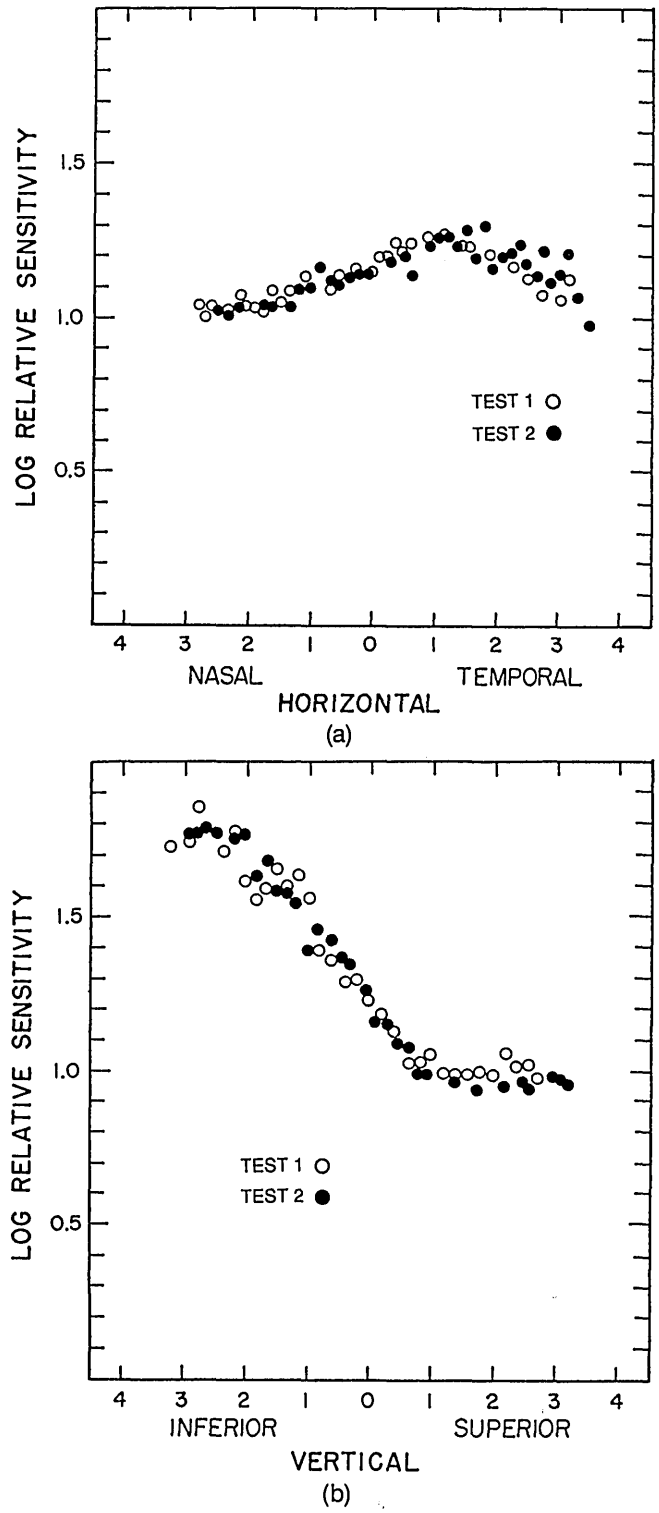

Fig. 5. (a) Graphical display of two horizontal SCE data sets illustrating a potential pitfall of limiting SCE data sampling to one pupillary meridian. Note the misleadingly flat SCE peaking 1.25 mm temporal. The circles represent data collection during two separate tests. Horizontal pupil entry is in millimeters. This figure is a reprint of Fig. VI-1 from Ref. 41. (b) Graphical display of two vertical SCE data sets for the same subject as in (a), illustrating a typical SCE spread (ρ value) with a markedly inferior displaced peak location. The marked flattening of the vertical SCE ~3 mm from the peak illustrates the limitation of fitting SCE data sets with parabolic functions beyond ±3 mm from the SCE peak location [see also Fig. 4(a)]. The circles represent data collection during two separate tests. Vertical pupil entry is in millimeters. This figure is a reprint of Fig. VI-2 from Ref. 41.

involvement in disease processes. For instance, patients with retinitis pigmentosa, diabetes, or age-related maculopathy often have cataract, which can render conventional models of the SCE effect useless. Applegate and Massof[34,42] demonstrated that the presence of cataract can be modeled by assuming that the cataract reduces log sensitivity in a Gaussian manner. Specifically, the model that they propose is

$$\log \eta = ax^2 + bx + c - A \exp[(x - d)^2/\sigma^2],$$

where the coefficients of the best-fitting curve (determined by an iterative least-squares analysis) estimate the density A, the location of maximum density d, and the spread σ of the cataract as well as the principal alignment tendencies $[-(b/2a)]$ and distributive properties $(-a)$ of the receptors being tested. Figure 7 graphically displays how the two-component model handles SCE data of a patient with a mild diffuse cataract. Figure 8 shows similar data for a patient with dense posterior subcapsular cataract.

NORMATIVE DATA GENERATION: EXPERIMENTAL

Apparatus

A standard two-channel Maxwellian-view optical system (Fig. 9) imaged two sources with unit magnification in the plane of the subject's entrance pupil. The sources (S_1 and S_2) were 1-mm pinholes transilluminated by red-light-emitting diodes having a peak luminous efficiency of 670 nm and a half-bandpass of 20 nm. The steady background beam from source S_1 entered the pupil in a fixed central location and provided the subject a view of a 7-deg, 30-troland circular background defined by aperture A_1. The test beam from source S_2 was electronically square-wave flickered at 2 Hz and provided the subject with a view of a 0.57-deg incremental test disk defined by aperture A_2 superimposed centrally upon the background. The pupillary entry point of the test beam in the plane of the entrance pupil was computer controlled by stepper motors, and its luminance was continuously variable over a 2-log-unit range.

Correction for the subject's refractive error (C) was placed in a translator and was adjusted to image sources S_1 and S_2 in the plane of the subject's entrance pupil when the vertex distance was fixed at 14 mm. Prismatic displacements of the test-beam pupil entry resulting from the refractive correction were calculated, and the position of the test source was corrected accordingly.

The subject's head position was fixed with both a dental bite mounted on a compound vise and a forehead rest. An alignment ring bearing a circle of evenly spaced small infrared luminous points centered on the optical axis of the apparatus was used to monitor the alignment of the eye to the apparatus. A beam splitter, BS_2, and a front surface mirror, FSM_2, optically conjugate with the subject's entrance pupil provided a near-focus video camera a view of the subject's pupil, the first Purkinje image of the alignment ring, and entry loci within the pupil of the test and background beam. Alignment was established and maintained to 0.10 mm by the experimenter's viewing the video output (magnified approximately ten times) on a monitor and adjusting the compound vise holding the bite-

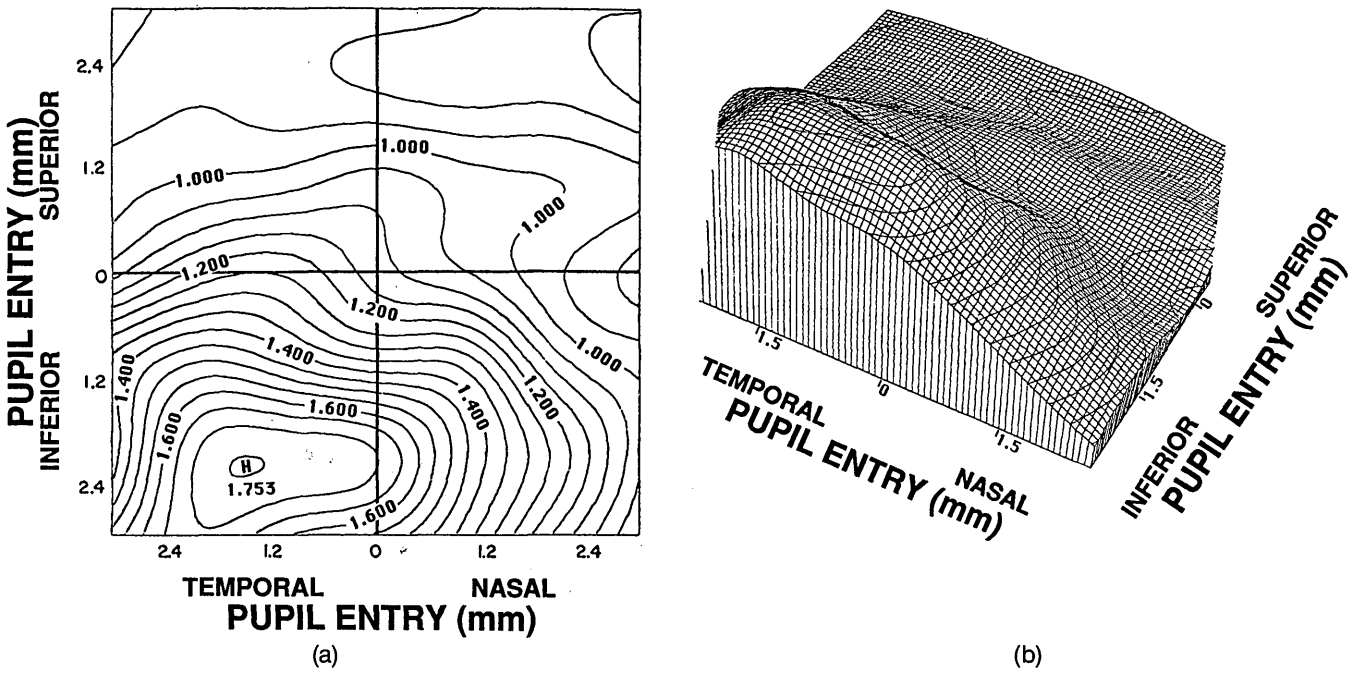

Fig. 6. (a) SCE displayed as a log sensitivity contour map calculated from SCE samples in seven evenly spaced pupillary meridians, illustrating the peak location of the SCE to be markedly inferior and nasal. The lines represent the horizontal and vertical pupillary meridians sampled in Figs. 5(a) and 5(b). Pupil entry is in millimeters. This figure is a reprint of Fig. VI-3 from Ref. 41. (b) Three-dimensional graphical display of the SCE contour map provides easy visualization of the peak location and the potential problems of limiting data sampling to a single pupillary meridian. This figure is a reprint of Fig. VI-4 from Ref. 41.

bar to maintain concentricity of the background beam image and the first Purkinje image of the alignment ring.

Subjects

Fifty-four optometry students between the ages of 22 and 35 years who were free of ocular or systemic disease and had best-corrected visual acuities of 20/20 or better served as subjects. Only right eyes were tested. Eyes were dilated before testing by use of one drop of 1% tropicamide ophthalmic solution and, if needed to obtain a full dilation, an additional drop of 10% phenylephrine hydrochloride ophthalmic solution. Foveal SCE for each subject for both horizontal and vertical pupil traverses of the test beam were measured in the laboratory of the first author.

Methods

Twenty-five pupillary entry points of the test beam were sampled at 0.25-mm steps along both the horizontal and vertical pupil meridians ±3 mm from the optical axis of the eye-apparatus system for a total of 50 data points. At each pupil-entry location the subject increased the luminance (if necessary) of the test disk until it was easily detected but not glaringly obvious and then, in turn, decreased the luminance of the test disk until the disk first disappeared. Thus sensitivity at each pupil entry was defined by use of a descending method of adjustment.

Parabolic smooth curves of the form given by Eq. (2) were fitted to both the horizontal and vertical SCE data sets by the method of least squares. Data points outside ±3 mm from the calculated SCE peak location were discarded, and the best-fitting parabola was recalculated by use of the reduced data set.

The accuracy with which the fitted function determines the peak of the SCE and its spread ρ is crucial to establishing norms because it is assumed that the central alignment and orientational tendencies are described by these parameters. Therefore the confidence intervals with which the data set fixes the peak and spread (ρ or $-a$) of the function were calculated by methods that were developed by Williams[43] and that were described for this application by Bedell.[44] Subjects having data sets with confidence intervals for ρ that were >0.01 were not considered to have generated valid data sets.

RESULTS

Normative Value of the SCE Peak Position and ρ Value

Aspects of these data have been presented previously.[45] Of the 54 eyes tested, 53 met the inclusion criteria of a 99% confidence interval for ρ of <0.01. Of these 53 subjects, 49 generated both horizontal and vertical data sets (four subjects failed to generate vertical data sets because of lack of time). Figure 10 graphically displays the peak location in both the horizontal and vertical pupillary meridians for the 49 eyes (circles) in which both horizontal and vertical effects were determined. The origin of Fig. 10 corresponds to the pupillary entry point at which the first Purkinje image is concentric with the optical axis of the apparatus with the eye fixing the test disk. The location of the first Purkinje image does not necessarily correspond with the center of the pupil. The square reflects the mean location of the horizontal (nasal 0.51 mm) and vertical (superior 0.20 mm) SCE peak locations, and the error bars reflect ±1 standard deviation (SD; horizontal ±0.72, vertical ±0.64).

Figure 11 graphically displays the horizontal and vertical ρ values at foveal fixation for the same 49 subjects. The square reflects the mean horizontal (0.047) and vertical (0.053) ρ values, and the error bars reflect ±1 SD (horizontal ±0.013, vertical ±0.012). The 45-deg diagonal

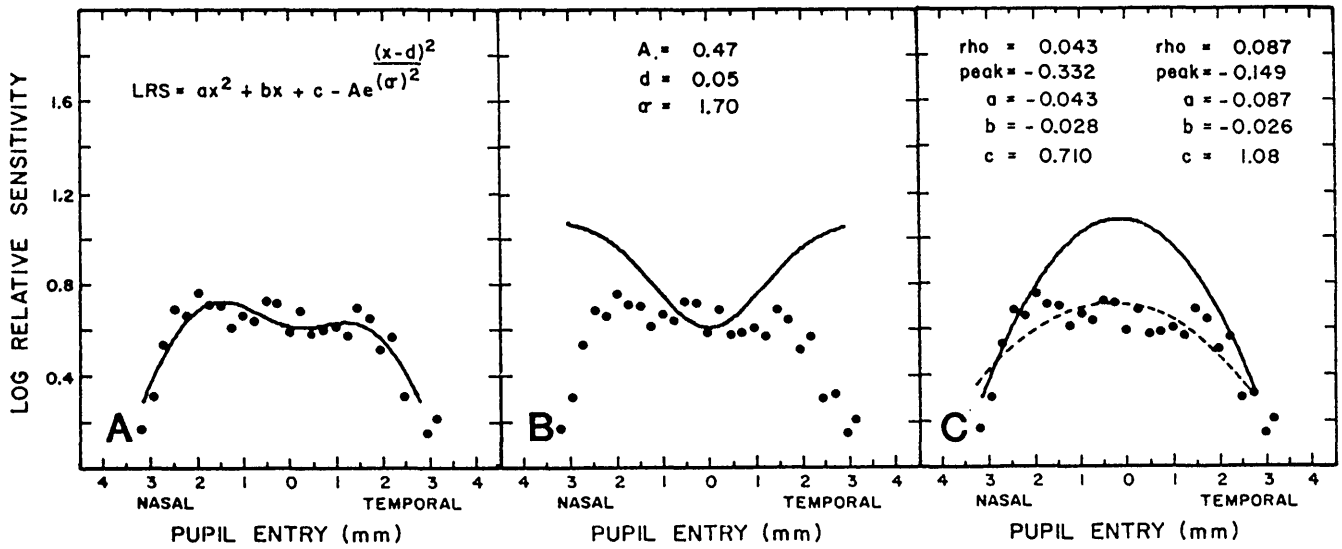

Fig. 7. Two-component model analysis of SCE behavior in a patient with a diffuse cataract: (a) the model's best-fitting function to the cataract-contaminated SCE data set; (b) the loss in log sensitivity resulting from the model's estimate of the cataract's maximum density A, peak location of maximum density d, and spread σ; (c) the two-component model's estimate of the best-fitting parabola (solid curve; coefficients listed in the right-hand corner) and the traditional single-component model's estimate of the best-fitting parabola (dashed curve; coefficients listed in the left-hand corner). This figure is a reprint of Fig. 5 from Ref. 34.

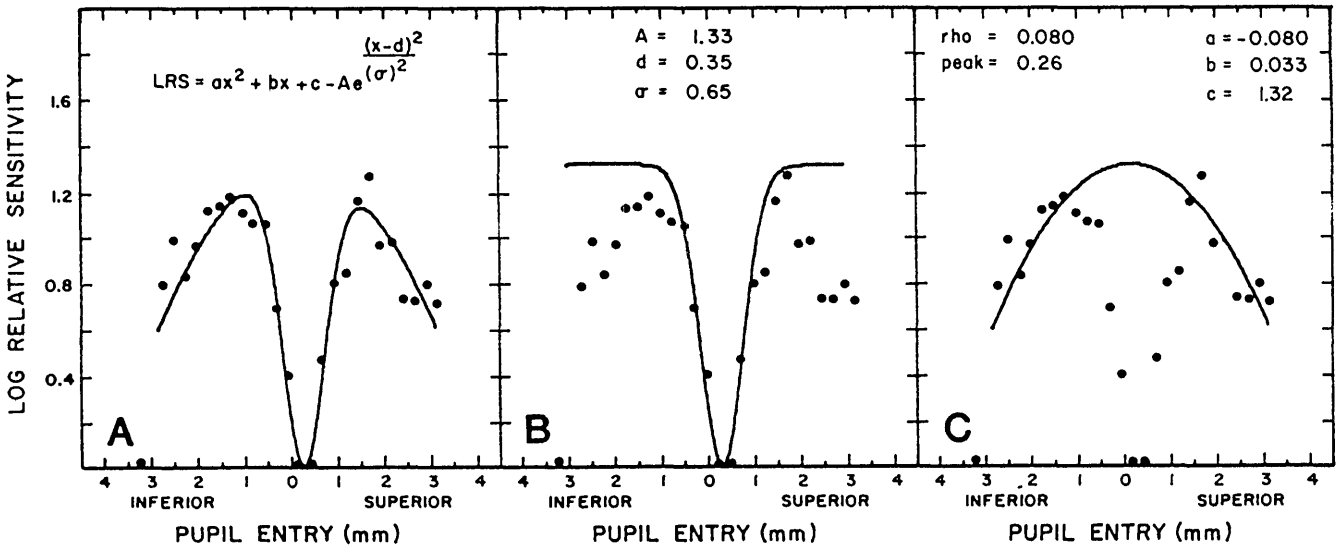

Fig. 8. Two-component model analysis of SCE behavior in a patient with a small dense posterior subcapsular cataract: (a) the model's best-fitting function to the cataract-contaminated SCE data set; (b) the loss in log sensitivity resulting from the model's estimate of the cataract's maximum density A, peak location of maximum density d, and spread σ; (c) the two-component model's estimate of the best-fitting parabola (curve; coefficients listed in the right-hand corner). The traditional single-component parabolic model cannot be meaningfully used to model this patient's measured SCE. This figure is a reprint of Fig. 8 from Ref. 34.

reflects the line along which data would be plotted if the horizontal and vertical ρ values were equal.

Other Studies and Combined Data

One other large study of the normal SCE peak location has been reported by Dunnewold.[46] In addition, several laboratories have reported the SCE results on small groups of normal subjects (e.g., Refs. 16 and 47–50). Only rarely have investigators reported their findings on SCE ρ values.

The comparison of SCE peak locations among studies is confounded by numerous factors, including differences in the entrance pupil reference point, which serves as the pupil-entry origin in graphical displays of the SCE. In some studies (such as this one) the pupillary reference point is the first Purkinje image. In others (such as that of Dunnewold[46]) the pupillary reference is the center of the dilated pupil. Despite the obvious potential for individual systematic variations in SCE peak location depending on the pupil reference selected, the group data of this paper (pupil reference, first Purkinje image) and those of Dunnewold[46] (pupil reference, center of dilated pupil) reveal essentially identical means and SD's for SCE peak location (Table 1). The fact that the SCE peak location in large samples is essentially independent of the pupil reference (dilated pupil center or first Purkinje image) and that the variation in the location of the two references across subjects is similar indicates that the locations of the first Purkinje image and the center of the dilated pupil

vary in a similar fashion and do not maintain a fixed relationship with respect to each other across subjects. Enoch and Hope[51] and Sorenson and Applegate[52] reached similar conclusions in studies comparing the relative locations of the dilated pupil, the constricted pupil, and the first Purkinje image across subjects.

Numerous studies have reported SCE peak locations and/or ρ values for one, two, or three normal eyes either graphically or in tabular form.[1,6,8,10,12,15,20,23-26,36,37,47-49,53-67] Occasionally studies will present mean values for SCE peak location and/or ρ value for five or more subjects and/or eyes.[16,50] We included in Tables 1 and 2 two studies reporting normative (but not individual) findings on five or more eyes as a separate entry. In the row labeled Enoch we included individual eyes across studies reported by the Enoch group.[15,20,23,37,47-49,54-59] In the row labeled Other we pooled all measurements across studies reporting SCE findings on individual normal eyes. In this other-studies data pool we included the individual eyes reported by Enoch's group (in the row labeled Enoch) but did not include the individual eyes reported by the two largest studies (that of Dunnewold and the present study). We were particularly careful to count data for each eye only once regardless of the number of times the data were reported. In the row labeled Combined we combined the SCE data for the individual eyes reported in this paper, in the Dunnewold study, and in the other-studies category (i.e., all studies reporting data on individual eyes). Data from the studies of Smith *et al.*[16] and Birch *et al.*[50] were not included because individual-eye data were not reported. Note that regardless of how the data are treated, the foveal SCE peak location in normal eyes is ~0.4 mm nasal and 0.2 mm superior to either the dilated-pupil center or the first Purkinje image and the foveal SCE ρ value is ~0.05 for either horizontal or vertical SCE data sets.

DISCUSSION

It is our hope that the normative data on SCE peak location and ρ value presented in this paper will be used to model the typical pupil-apodization function for the human eye. Furthermore, since the SCE is an excellent means for monitoring the integrity of the photoreceptor layer, we are particularly hopeful that the normative data presented will be helpful in the study of photoreceptor involvement in retinal pathology.

Although the SCE gives insight to receptor involvement in known retinal pathology (e.g., Refs. 15, 17, 19, 46, 50, and 68–74), it has received relatively limited attention in clinical applications generally and almost no application as a tool for early detection and/or prediction of impending photoreceptor involvement in disease processes. There are four main factors limiting the utilization of SCE measurement in the clinical setting: (1) the measurement is extremely local; (2) measurement techniques are too time consuming; (3) the measurement generally requires a subjective response from an untrained observer; and (4) there is a lack of large sample normative data, particularly with respect to ρ.

The normative data presented above should contribute greatly toward solving the need for a normative data base. However, as in most clinical measures, the variation within the reference population (because of measurement error and variability among subjects) is large compared with the variation in repeated measures on a single individual.[19,54,75] For example, data from Fig. 4 of Applegate and Bonds[19] demonstrate that each individual-eye data set of a trained subject locates the SCE peak with a 99% confidence interval of better than ±0.20 mm, whereas the average of five measures of SCE peak location from five determinations of the SCE (one per day for five days)

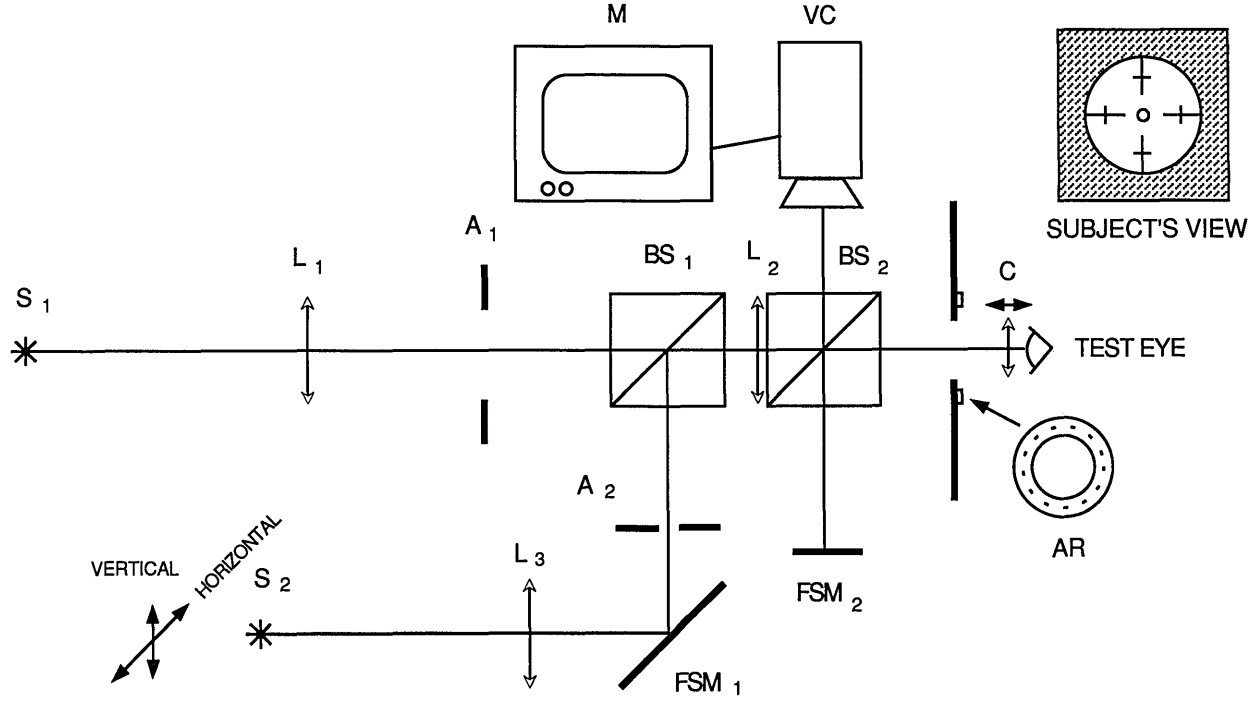

Fig. 9. Schematic of the two-channel Maxwellian-view system used to generate normative data (its operation is described in the text): S's, sources; A's, apertures; BS's, beam splitters; L's, lenses; AR, alignment ring; FSM's, front surface mirrors; C, refractive correction; VC, video camera; M, monitor.

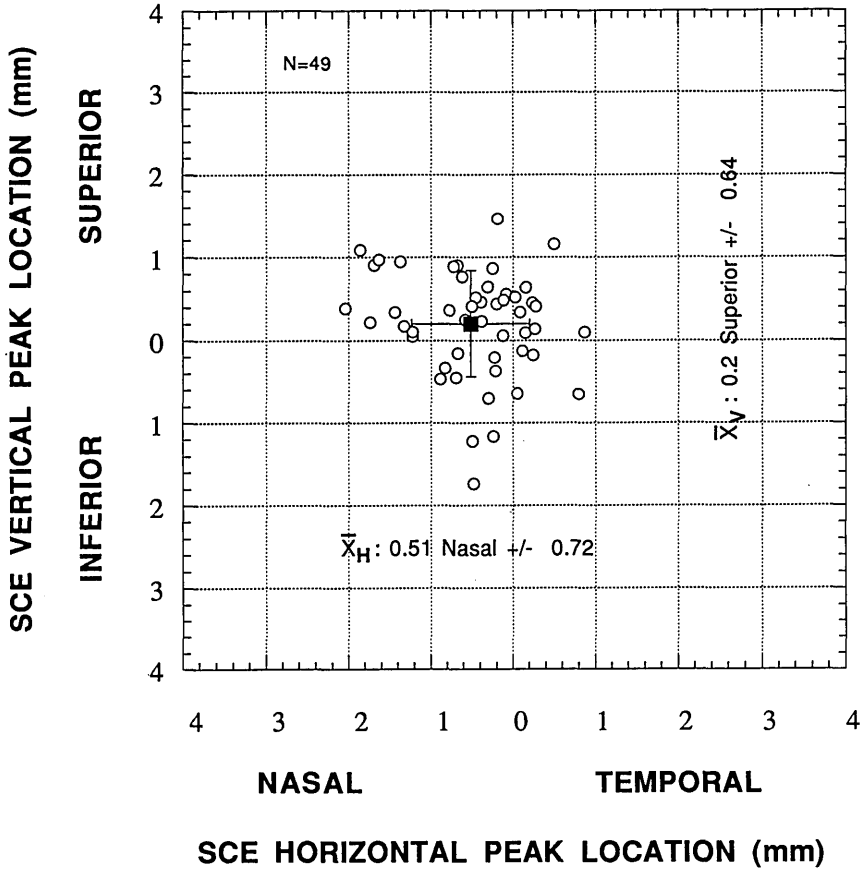

Fig. 10. SCE horizontal and vertical peak locations for the right eyes of 49 normal subjects (circles). The square represents the average peak location, and the error bars reflect ±1 SD.

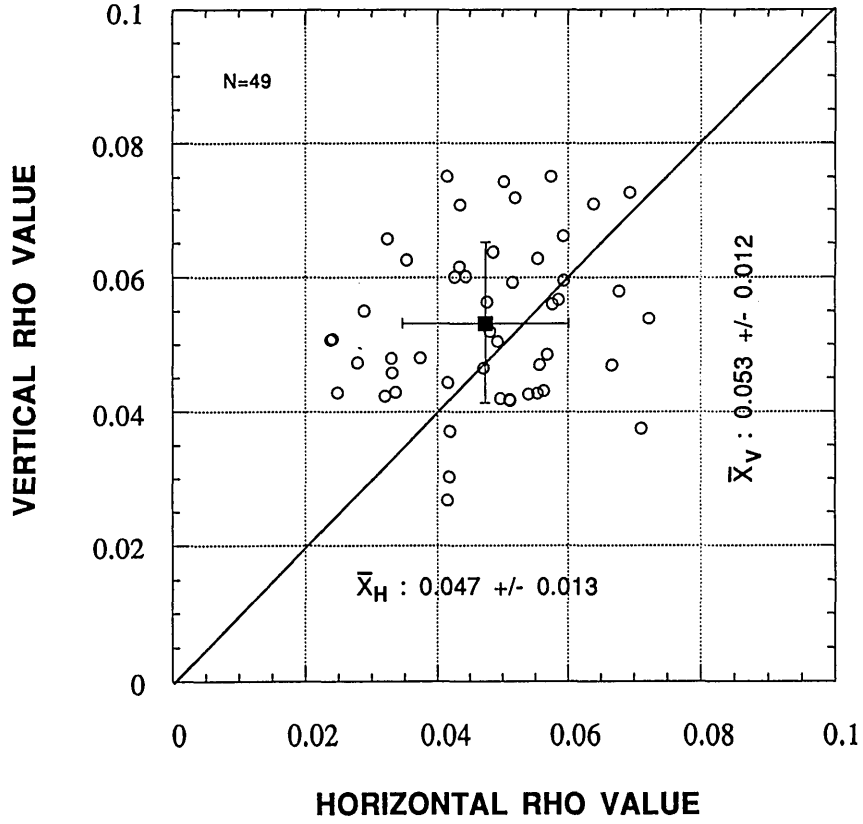

Fig. 11. SCE horizontal and vertical ρ values for the right eyes of 49 normal subjects (circles). The square represents the average ρ value, and the error bars reflect ±1 SD. There is a slight nonsignificant tendency for the vertical ρ value to be greater than the horizontal ρ value, as indicated by the majority of the data falling above the diagonal of slope equal to 1.0.

Table 1. Normative Data for SCE Peak Location

Study/Reference		Horizontal			Vertical		
First Author	Pupil Reference	Number of Studies	Number of Subjects/Eyes	Peak ±1 SD (Nasal)	Number of Studies	Number of Subjects/Eyes	Peak ±1 SD (Superior)
Applegate	First Purkinje	1	49/49 RE[a]	0.47 ± 0.68	1	49/49 RE	0.20 ± 0.64
			53/53 RE	0.51 ± 0.72			
			18/18 RE	0.46 ± 0.67		18/18 RE	0.17 ± 0.80
Dunnewold	Pupil Center	1	18/18 LE[b]	0.27 ± 0.84	1	18/18 LE	0.61 ± 0.90
			29/47 RE/LE[c]	0.37 ± 0.78		29/47 RE/LE	0.29 ± 0.80
Enoch		12	29/29 RE/LE	0.25 ± 0.40	7	20/20 RE/LE	0.14 ± 0.44
Birch		1	5/5 RE/LE	0.4	–	–	–
Other[d]	Mixed	31	69/69 RE/LE	0.32 ± 0.61	12	31/31 RE/LE	0.09 ± 0.37
Combined	Mixed	33	151/169 RE/LE	0.40 ± 0.70	14	109/127 RE/LE	0.20 ± 0.66

[a]Right eyes.
[b]Left eyes.
[c]Right and left eyes.
[d]Includes Enoch.

Table 2. Normative Data for SCE ρ Values

Study/Reference		Horizontal			Vertical		
First Author	Pupil Reference	Number of Studies	Number of Subjects/Eyes	ρ ± SD	Number of Studies	Number of Subjects/Eyes	ρ ±1 SD
Applegate	First Purkinje	1	49/49 RE[a]	0.048 ± 0.013	1	49/49 RE	0.053 ± 0.012
			53/53 RE	0.047 ± 0.013			
Smith		1	7/7 RE/LE[b]	0.046 ± 0.003	–	–	–
Enoch		6	15/15 RE/LE	0.045 ± 0.012	3	6/6 RE/LE	0.036 ± 0.011
Birch		1	5/5 RE/LE	0.050	–	–	–
Other[c]	Mixed	7	18/18 RE/LE	0.047 ± 0.012	4	9/9 RE/LE	0.046 ± 0.018
Combined	Mixed	8	71/71 RE/LE	0.047 ± 0.013	5	58/58 RE/LE	0.052 ± 0.013

[a]Right eyes.
[b]Right and left eyes.
[c]Includes Enoch.

locates the peak with a SD of ±0.06 mm. Thus individuals can exhibit abnormal changes in their SCE's and not fall outside group norms. To our knowledge no repeated-measure norms for SCE parameters have been generated on inexperienced subjects. The availability of such norms would be a particularly useful reference for monitoring a patient's photoreceptor involvement early in a disease process and over time.

Measurement speed can be increased by using efficient data-collection routines and clever stimuli.[14,19,57] However, even for the so-called fast SCE measurement techniques, sampling multiple retinal locations in an effort to detect or predict impending photoreceptor involvement in pathology is neither time effective nor cost effective. On the other hand, if the retinal location of interest is known, as in age-related maculopathy (the leading cause for legal blindness over the age of 50 years[76,77]), the SCE measurement can be quite useful in early detection of photoreceptor involvement.[16,34]

Perhaps the single biggest breakthrough for the clinical application of the SCE would be the development of a fast, objective measurement method for quantifying the effect. Such a method should be able to generate objective data for the retinal locus of interest in less than a minute, should require only a simple chin-and-forehead rest for eye stabilization, and should immediately produce analyzed results suitable for the clinical record. Such an objective method is not impossible. Employing principles of reflectomodulometry to measure the directional sensitivity of the retina objectively, Gorrand and Delori,[78] Burns *et al.*,[79] and Gorrand[80] recently measured functions that appear to mimic closely psychophysically measured SCE in <15 s across the entire pupil.

In summary, normative data reveal that the foveal SCE peak location and ρ value maintain essentially constant values across laboratories. Specifically, in our laboratory, using the largest population of individual eyes from individual untrained subjects reported to date, we find the SCE peak location to be 0.51 nasal (53 normal eyes in 53 individuals) and 0.20 superior (49 normal eyes in 49 individuals), with SD's of ±0.72 and ±0.64, respectively, and the SCE ρ value for the same eyes to be 0.047 horizontally and 0.053 vertically, with SD's of ±0.013 and ±0.012, respectively. Combining data across all studies, we find the SCE peak location to be 0.40 nasal (151 normal eyes in 169 individuals) and 0.20 superior (109 normal eyes in 127 individuals), with SD's of ±0.70 and ±0.66, respectively, and the SCE ρ value to be 0.047 horizontally (71 normal eyes in 71 individuals) and 0.052 vertically (58 normal eyes in 58 individuals), with SD's of ±0.013 and ±0.013, respectively.

ACKNOWLEDGMENTS

This research was supported by National Institutes of Health National Eye Institute grant EY08520 and a San Antonio Area Foundation grant (to R. A. Applegate) and by an unrestricted research grant to the Department of

Ophthalmology, University of Texas Health Science Center at San Antonio, from Research to Prevent Blindness, Inc., New York, N.Y. We thank Christina M. Sorenson and Diana Meade Scoggins for data collection and analysis, Preeti Nair for summary-data organization and presentation, and Tracy Hurd for word processing and manuscript organization.

REFERENCES

1. W. S. Stiles and B. H. Crawford, "The luminous efficiency of rays entering the eye pupil at different points," Proc. R. Soc. London Ser. B **112,** 428–450 (1933).
2. J. M. Enoch and F. L. Tobey, eds., *Vertebrate Photoreceptor Optics*, Vol. 23 of Springer Series in Optics Science (Springer-Verlag, Berlin, 1981).
3. J. M. Enoch and V. Lakshminarayanan, "Retinal fiber optics, in *Vision and Visual Dysfunction*, N. Charman, ed. (Macmillan, London, 1991), Vol. 1, pp. 280–309.
4. R. A. Weale, "Notes on the photometric significance of the human crystalline lens," Vision Res. **1,** 183–191 (1961).
5. J. Mellerio, "Light absorption and scatter in the human lens," Vision Res. **11,** 129–141 (1971).
6. B. H. Crawford, "The luminous efficiency of light entering the eye pupil at different points and its relation to brightness threshold measurement," Proc. R. Soc. London Ser. B **124,** 81–96 (1937).
7. J. A. VanLoo and J. M. Enoch, "The scotopic Stiles–Crawford effect," Vision Res. **15,** 1005–1009 (1975).
8. G. Westheimer, "Dependence of the magnitude of the Stiles–Crawford effect on retinal location," J. Physiol. London **192,** 309–315 (1967).
9. D. van Norren and J. van der Kraats, "A continuously recording retinal densitometer," Vision Res. **21,** 897–905 (1981).
10. G. J. van Blokland, "Directionality and alignment of the foveal receptors, assessed with light scattered from the human fundus *in vivo*," Vision Res. **26,** 495–500 (1986).
11. H. H. Ripps and R. A. Weale, "Photolabile changes and the directional sensitivity of the human fovea," J. Physiol. (London) **173,** 57–64 (1964).
12. J. R. Coble and W. A. H. Rushton, "Stiles–Crawford effect and the bleaching of cone pigments," J. Physiol. London **217,** 231–242 (1971).
13. A. M. Laties, "Histological techniques for study of photoreceptor orientation," Tissue Cell **1,** 63–81 (1969).
14. K. Blank, R. R. Provine, and J. M. Enoch, "Shift in the peak of the photopic Stiles–Crawford function with marked accommodation," Vision Res. **15,** 499–507 (1975).
15. J. M Enoch, J. A. VanLoo, and E. Okun, "Realignment of photoreceptors disturbed in orientation secondary to retinal detachment," Invest. Ophthalmol. **12,** 849–853 (1973).
16. V. C. Smith, J. Pokorny, and K. R. Diddie, "Color matching and the Stiles–Crawford effect in observers with early age-related macular changes," J. Opt. Soc. Am. **5,** 2113–2121 (1988).
17. V. C. Smith, J. Pokorny, J. T. Ernest, and S. J. Starr, "Visual function in acute posterior multifocal placoid pigment epitheliopathy," Am. J. Ophthalmol. **85,** 192–199 (1978).
18. P. Kinnear, M. Marre, J. Pokorny, V. C. Smith, and G. Verriest, "Specialized methods of evaluating color vision defects," in *Congenital and Acquired Color Vision Defects*, J. Pokorny, V. C. Smith, G. Verriest, and A. J. L. G. Pinckers, eds. (Grune & Stratton, New York, 1979), pp. 137–181.
19. R. A. Applegate and A. B. Bonds, "Induced movement of receptor alignment toward a new pupillary aperture," Invest. Ophthalmol. Vis. Sci. **21,** 869–873 (1981).
20. J. M. Enoch and D. G. Birch, "Inferred positive phototropic activity in human photoreceptors," Philos. Trans. R. Soc. London Ser. B **291,** 323–351 (1981).
21. W. S. Stiles, "The luminous efficiency of monochromatic rays entering the eye pupil at different points and a new color effect," Proc. R. Soc. London Ser. B **123,** 90–118 (1937).
22. P. Moon and D. Spencer, "On the Stiles–Crawford effect," J. Opt. Soc. Am. **34,** 319–329 (1944).
23. J. M. Enoch, "Summated response of the retina to light entering different parts of the pupil," J. Opt. Soc. Am. **48,** 392–405 (1958).
24. A. Safir and L. Hyams, "Distribution of cone orientations as an explanation for the Stiles–Crawford effect," J. Opt. Soc. Am. **59,** 757–765 (1969).
25. A. Safir, L. Hyams, and J. Philpot, "The retinal directional effect: a model based on the Gaussian distribution of cone orientations," Vision Res. **11,** 819–831 (1971).
26. G. A. Geri, G. L. Kandel, C. R. Genter, and H. E. Breed, "Meridional differences in the directional sensitivity of human color mechanisms," Am. J. Optom. Physiol. Opt. **65,** 880–889 (1988).
27. V. Lakshminarayanan and J. M. Enoch, "Shape of the Stiles–Crawford function for traverses of the entrance pupil not passing through the peak of sensitivity," Am. J. Optom. Physiol. Opt. **62,** 127–128 (1985).
28. V. Lakshminarayanan, J. E. Bailey, and J. M. Enoch, "The optics of phakic, pseudophakic, and aphakic eyes: effects on the Stiles–Crawford function," Optom. Vis. Sci. (to be published).
29. A. Safir, L. Hyams, and J. Philpot, "Movement of the Stiles–Crawford effect," Invest. Ophthalmol. Vis. Sci. **9,** 820–825 (1971).
30. J. M. Enoch and H. E. Bedell, "Specification of the directionality of the Stiles–Crawford function," Am. J. Optom. Physiol. Opt. **56,** 341–344 (1979).
31. G. Toraldo di Francia, "The radiation pattern of retinal receptors," Proc. Phys. Soc. London Ser. B **62,** 461–462 (1949).
32. J. M. Enoch, "Vertebrate rod receptors are directionally sensitive," in *Photoreceptor Optics*, A. W. Snyder and R. Menzel, eds. (Springer-Verlag, Berlin, 1975), pp. 17–37.
33. F. L. Tobey, J. M. Enoch, and J. H. Scandrett, "Experimentally determined optical properties of goldfish cones and rods," Invest. Ophthalmol. **14,** 7–23 (1975).
34. R. A. Applegate and R. W. Massof, "The Stiles–Crawford effect in retinal disease: interpretation in the presence of cataract," in *Vision Science Symposium: A Tribute to Gordon G. Heath* (Indiana U. Press, Bloomington, Ind., 1988), pp. 27–45.
35. V. Lakshminarayanan and M. L. Calvo, "Initial field and energy flux in absorbing optical waveguides. II. Implications," J. Opt. Soc. Am. A **4,** 2133–2140 (1987).
36. D. I. A. MacLeod, "Directionally selective light adaptation: a visual consequence of receptor disarray?" Vision Res. **14,** 369–378 (1974).
37. R. D. Hamer, V. Lakshminarayanan, J. M. Enoch, and J. J. O'Donnell, "Selective adaptation of the Stiles–Crawford function in a patient with gyrate atrophy," Clin. Vis. Sci. **1,** 103–106 (1986).
38. D. G. Birch and M. A. Sandberg, "Psychophysical studies of cone optical bandwidth in patients with retinitis pigmentosa," Vision Res. **22,** 1113–1117 (1982).
39. J. E. Bailey, V. Lakshminarayanan, and J. M. Enoch, "The Stiles–Crawford function in an aphakic subject with retinitis pigmentosa," Clin. Vis. Sci. **6,** 165–170 (1991).
40. V. Lakshminarayanan and J. M. Enoch, "The MacLeod selective adaptation paradigm in cases with modest cataracts," Clin. Vis. Sci. **3,** 155–156 (1988).
41. R. A. Applegate, "Aperture effects on phototropic orientation properties of human photoreceptors," Ph.D. dissertation (University of California, Berkeley, Berkeley, Calif., 1983).
42. R. A. Applegate and R. W. Massof, "Interpreting the Stiles–Crawford effect in patients with cataracts," in *Noninvasive Assessment of the Visual System*, Vol. 6 of 1985 OSA Technical Digest Series (Optical Society of America, Washington, D.C., 1985), pp. WA6-1–WA6-4.
43. E. J. Williams, *Regression Analysis* (Wiley, New York, 1959).
44. H. E. Bedell, "Retinal receptor orientation in amblyopic and nonamblyopic eyes assessed at several retinal locations using the psychophysical Stiles–Crawford function," Ph.D. dissertation (University of Florida, Gainesville, Fla., 1978).
45. R. A. Applegate, D. L. Meade, and C. M. Sorenson, "Normal variation in the Stiles–Crawford function," in *Noninvasive Assessment of the Visual System*, Vol. 4 of 1987 OSA Technical Digest Series (Optical Society of America, Washington, D.C., 1987, pp. MA4-1–MA4-4.

46. C. J. W. Dunnewold, "On the Campbell and Stiles–Crawford effects and their clinical importance," Ph.D. dissertation (Rijksuniversiteit te Utrecht, Utrecht, The Netherlands, 1964), pp. 1–84.
47. J. M. Enoch and G. M. Hope, "Directional sensitivity of the foveal and parafoveal retina," Invest. Ophthalmol. **12,** 497–503 (1973).
48. J. M. Enoch and G. M. Hope, "An analysis of retinal receptor orientation. III. Results of initial psychophysical tests," Invest. Ophthalmol. **11,** 765–782 (1972).
49. J. M. Enoch, "Further studies on the relationship between amblyopia and the Stiles–Crawford effect," Am. J. Optom. Arch. Am. Acad. Optom. **36,** 111–128 (1959).
50. D. G. Birch, M. A. Sandberg, and E. L. Berson, "The Stiles–Crawford effect in retinitis pigmentosa," Invest. Ophthalmol. Vis. Sci. **22,** 157–164 (1982).
51. J. M. Enoch and G. M. Hope, "An analysis of retinal receptor orientation. IV. Center of the entrance pupil and the center of convergence of orientation and directional sensitivity," Invest. Ophthalmol. **11,** 1017–1021 (1972).
52. C. M. Sorenson and R. A. Applegate, "The location of the Stiles–Crawford peak and the centers of the dilated and naturally constricted pupil," Am. J. Optom. Physiol. Opt. **60,** 26 (1983).
53. F. Flamant and W. S. Stiles, "The directional and spectral sensitivities of the retinal rods to adapting fields of different wave-lengths," J. Physiol. (London) **107,** 187–202 (1947).
54. H. E. Bedell and J. M. Enoch, "A study of the Stiles–Crawford function at 35 degrees in the temporal field and the stability of the foveal Stiles–Crawford function over time," J. Opt. Soc. Am. **69,** 435–442 (1979).
55. H. E. Bedell, J. M. Enoch, and C. R. Fitzgerald, "Photoreceptor orientation: a graded disturbance bordering a region of choroidal atrophy," Arch. Ophthalmol. **99,** 1841–1844 (1981).
56. J. M. Enoch, R. D. Hamer, V. Lakshminarayanan, T. Yasuma, D. G. Birch, and S. Yamade, "Effect of monocular light exclusion on the Stiles–Crawford function," Vision Res. **27,** 507–510 (1987).
57. S. Yamade, V. Lakshminarayanan, and J. M. Enoch, "Comparison of two fast quantitative methods for evaluating the Stiles–Crawford function," Am. J. Optom. Physiol. Opt. **64,** 621–626 (1987).
58. J. M. Enoch, "Marked accommodation, retinal stretch, monocular space perception and retinal receptor orientation," Am. J. Optom. Physiol. Opt. **52,** 375–392 (1975).
59. J. M. Enoch and D. G. Birch, "Evidence for alteration in photoreceptor orientation," Ophthalmology **87,** 821–834 (1980).
60. J. J. Vos and A. Huigen, "A clinical Stiles–Crawford apparatus," Am. J. Optom. Arch. Am. Acad. Optom. **39,** 68–76 (1962).
61. W. D. Wright and J. H. Nelson, "The relation between the apparent intensity of a beam of light and the angle at which the beam strikes the retina," Proc. Phys. Soc. London **48,** 401–405 (1936).
62. M. Aguilar and A. Plaza, "Effecto Stiles–Crawford en vision extrafoveal," An. R. Soc. Esp. Fis. Quim. **50,** 119–126 (1954).
63. A. M. Ercoles, L. Ronchi, and G. Toraldo di Francia, "The relation between pupil efficiencies for small and extended pupils of entry," Opt. Acta **3,** 84–89 (1956).
64. C. F. Goodeve, "Relative luminosity in the extreme red," Proc. E. Soc. London Ser. A **155,** 644–683 (1936).
65. N. O. Miller, "The changes in Stiles–Crawford effect with high luminance adapting fields," Am. J. Optom. **41,** 599–608 (1964).
66. B. O'Brien, "A theory of the Stiles–Crawford effect," J. Opt. Soc. Am. **36,** 506–509 (1946).
67. J. E. Bailey and G. G. Heath, "Flicker effects of receptor directional sensitivity," Am. J. Optom. Physiol. Opt. **55,** 807–812 (1978).
68. F. Fankhauser, J. M. Enoch, and P. Cibis, "Receptor orientation in retinal pathology," Am. J. Ophthalmol. **52,** 767–783 (1961).
69. C. R. Fitzgerald, D. G. Birch, and J. M. Enoch, "Functional analysis of vision in patients following retinal detachment repair," Arch. Ophthalmol. **98,** 1237–1244 (1980).
70. V. C. Smith, J. Pokorny, and K. R. Diddie, "Color matching and Stiles–Crawford effect in central serous choroidopathy," Mod. Probl. Ophthalmol. **19,** 284–295 (1978).
71. J. Pokorny, V. C. Smith, and J. T. Ernest, "Macular color vision defects: specialized psychophysical testing in acquired and hereditary choroiretinal diseases," Int. Ophthalmol. Clin. **20,** 53–81 (1980).
72. E. C. Campos, H. E. Bedell, J. M. Enoch, and C. R. Fitzgerald, "Retinal receptive field-like properties and Stiles–Crawford effect in a patient with traumatic choroidal rupture," Doc. Ophthalmol. **45,** 381–395 (1978).
73. H. E. Bedell, J. M. Enoch, and C. R. Fitzgerald, "A graded disturbance bordering a region of choroidal atrophy," Arch. Ophthalmol. **99,** 1841–1844 (1981).
74. J. Pokorny, V. C. Smith, and P. B. Johnston, "Photoreceptor misalignment accompanying a fibrous scar," Arch. Ophthalmol. **97,** 867–869 (1979).
75. W. S. Stiles, "The directional sensitivity of the retina and the spectral sensitivities of the rods and cones," Proc. R. Soc. London Ser. B **127,** 64–105 (1939).
76. *Summary and Critique of Available Data on the Prevalence and Economic and Social Costs of Visual Disorders and Disabilities* (Westat, Inc., Rockville, Md., 1976).
77. A. Sorsby, *The Incidence and Causes of Blindness in England and Wales. Reports on Public Health and Medical Subjects* (H. M. Stationary Office, London, 1966).
78. J. M. Gorrand and F. C. Delori, "A method for assessing photoreceptor directionality," Invest. Ophthalmol. Vis. Sci. Suppl. **31,** 425 (1990).
79. S. A. Burns, A. E. Elsner, J. M. Gorrand, and M. R. Kreitz, "Variability in color matching, photoreceptor alignment, and the Stiles–Crawford II effect, in *Annual Meeting,* Vol. 17 of 1991 OSA Technical Digest Series (Optical Society of America, Washington, D.C., 1991), p. 24.
80. J. M. Gorrand, "Use of reflecto-modulometry to study the optical quality of the inner retina," Ophthalmic Physiol. Opt. **9,** 198–204 (1989).